Voltage-Dependent Properties of Three Different Gating Modes in Single Cardiac Na^+ Channels

Thomas Böhle and Klaus Benndorf
Department of Physiology, University of Cologne, D-50931 Cologne, Germany

ABSTRACT Three different modes of Na^+ channel action, the F mode (fast-inactivating), the S mode (slowly inactivating), and the P mode (persistent), were studied at different potentials in exceptionally small cell-attached patches containing one and only one channel. Switching between the modes was independent of voltage. In the F mode, the mean open time (τ_o) at −30 and −40 mV was 0.14 and 0.16 ms, respectively, which was significantly larger than at −60 and 0 mV, where the values were 0.07 and 0.08 ms, respectively. The time before which half of the first channel openings occurred ($t_{0.5}$), decreased from 0.58 ms at −60 mV to 0.14 ms at 0 mV. The fit of steady-state activation with a Boltzmann function yielded a half-maximum value ($V_{0.5}$) at −48.1 mV and a slope (k) of 5.6 mV. The mean open time in the S mode increased steadily from 0.12 ms at −80 mV to 1.09 ms at −30 mV, but was not prolonged further at −20 mV (1.07 ms). Concomitantly, $t_{0.5}$ decreased from 1.61 ms at −80 mV to 0.22 ms at −20 mV. Here the midpoint of steady-state activation was found at −61.2 mV, and the slope was 8.7 mV. The mean open time in the P mode increased from 0.07 ms at −60 mV to 0.45 ms at 0 mV and $t_{0.5}$ declined from 2.14 ms at −60 mV to 0.19 ms at +20 mV. Steady-state activation had its midpoint at −14.7 mV, and the slope was 10.9 mV. It is concluded that a single Na^+ channel may switch among the F, S, and P mode and that the three modes differ by a characteristic pattern of voltage dependence of τ_o, $t_{0.5}$, and steady-state activation.

INTRODUCTION

In cardiac muscle, voltage-dependent Na^+ channels are responsible for the fast depolarizing phase of the action potential (Lee et al., 1979; Brown et al., 1981; Cachelin et al., 1983; grant et al., 1983; Kunze et al., 1985). However, considerable evidence exists that Na^+ channels become activated also during later phases of the action potential (Attwell et al., 1979; Carmeliet, 1984, 1987; Patlak and Ortiz, 1985; Kohlhardt et al., 1987). In single beating cells of chick-embryo heart, four different types of Na^+ channel action were identified and correlated to different phases of the action potential by direct measurement (Liu et al., 1992; Mazzanti and DeFelice, 1987; Wellis et al., 1990): 1) the fast-inactivating Na^+ current during the upstroke of the action potential, 2) the outward Na^+ current, positive to the dynamic Na^+ reversal potential after the upstroke, lasting for 30 to 40 ms, 3) the rare, isolated, brief, and 4) the rare, long-lasting events that both occur during the action-potential plateau. It is still unclear whether these Na^+ currents are carried by different types of Na^+ channel molecules or represent different modes of Na^+ channel action.

By using patch pipettes with exceptionally small pores and thick walls (Benndorf, 1995), voltage-dependent Na^+ currents in cell-attached patches containing one and only one channel could be recorded at low noise in myocardial mouse cells. Recently, we reported with this technique the existence of five distinct gating modes of Na^+ channel action (Böhle and Benndorf, 1995). These are the fast-inactivating (F), the intermediate 1 (M1), the intermediate 2 (M2), the slow (S), and the persistent (P) mode, as named by the time course of macroscopic inactivation. The lifetime of the modes, determined from the long-time course of the averaged current per trace, is variable, being in the range of some seconds (lower boarder of identification) to several minutes. Each mode has a characteristic mean open-channel life time τ_o and distribution of first latency. At −40 mV, the F mode has a short mean open time ($\tau_o \approx 0.16$ ms) and a short first latency (the time before which half of the first channel openings occurred, $t_{0.5} \approx 0.2$ ms), the S mode has a long mean open time ($\tau_o \approx 1.01$ ms) and a short first latency ($t_{0.5} \approx 0.3$ ms), and the P mode has a short mean open time ($\tau_o \approx 0.13$ ms) and a long first latency ($t_{0.5} \approx 1.2$ ms). In this study, we focus on the voltage dependence of open-time distribution, first-latency distribution, and steady-state activation of the F, S, and P mode.

MATERIALS AND METHODS

Cell preparation, temperature, and solutions

Single cells of heart ventricles from adult white mice were isolated according to the procedure described by Benndorf (1993). The experiments were performed at room temperature (22–24°C) in a bathing solution that contained the following (in mmol/l): 230 KCl, 20 CsCl, 1 $MgCl_2$, 10 EGTA, 5 HEPES, pH 7.3, and a pipette solution that contained (in mmol/l) 255 NaCl, 2.5 $CaCl_2$, 4 KCl, 5 HEPES, pH 7.3. The elevated Na^+ concentration was used to enhance unitary current amplitudes (Yue et al., 1989).

Patch pipettes

Patch pipettes were prepared from thick-walled (external diameter, 2.0 mm; internal diameter 0.5 mm) borosilicate glass tubing (Hilgenberg, Malsfeld, Germany) for the purpose of low-noise recording as described in

Received for publication 7 February 1995 and in final form 8 May 1995.

Address reprint requests to Thomas Böhle, Department of Physiology, University of Cologne, Robert-Koch-Strasse 39, D-50931 Cologne, Germany. Tel.: 221-478-6951; Fax: 221-478-6965.

K. Benndorf is a Heisenberg fellow of the Deutsche Forschungsgemeinschaft.

0006-3495/95/09/873/10 $2.00

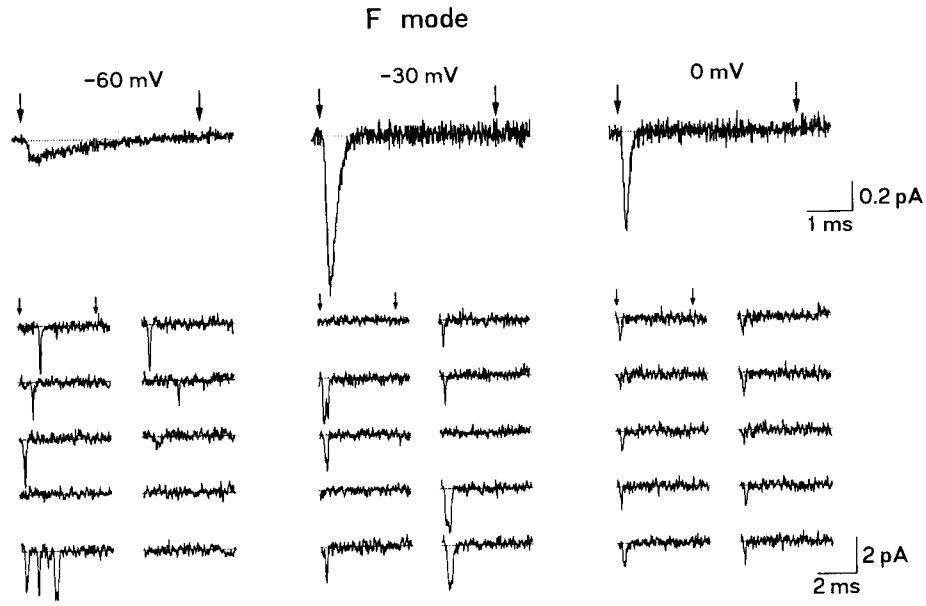

FIGURE 1 Typical currents of a Na^+ channel gating in the F mode at three different potentials (patch 1, pipette resistance 50 MΩ; seal resistance, 14 GΩ; holding potential, −130 mV, no prepulses; the arrows indicate beginning and end of the test pulses). (*bottom*) 10 consecutive sweeps (filter 5 kHz) are shown at each potential. (*top*) The ensemble-averaged currents are shown, which were formed from 1016 traces at −60 mV, 1019 traces at −30 mV, and 1001 traces at 0 mV (filter 20 kHz).

detail by Benndorf (1995) and were inserted into a pipette holder of small dimensions (Benndorf, 1993). A special technique, in which pipette tips were generated only seconds before the actual gigaohm-seal formation by breaking off the tip region (Böhle and Benndorf, 1994), was used in part of the experiments. Gigaohm seals were normally obtained by application of slight suction.

Data acquisition and analysis

Unitary Na^+ currents were recorded at a sampling rate of 66 or 100 kHz in the cell-attached patch configuration with an AXOPATCH 200A amplifier (integrating headstage, intrinsic noise 0.068 pA rms at 5 kHz, Axon Instruments, Foster City, CA). Analog filtering was performed with an 8-pole Bessel-filter at a band width of 20 kHz (48 dB/octave, Frequency Devices, Haverhill, MA). When data needed further filtering for the analysis, an off-line Gaussian filter algorithm was used. If not otherwise noted, the holding potential was −120 mV, and pulses of 4-ms duration to various potentials ranging from −100 to +20 mV were applied at a rate of 20 Hz from a prepulse potential of −180 mV, at which the patch was held for 20 ms to completely remove fast inactivation. The mode-specific and potential-dependent open probability was constant. It is concluded, therefore, that despite the high pulsing rate restoration from slow inactivation of the Na^+ channels was complete. Capacitive transients were compensated carefully via compensation circuits containing in summary four exponentials. Leakage and remaining capacitive currents were removed by subtracting averaged blank traces, which were formed exclusively from traces in the neighborhood of the actual sweep. None of the patches in the present study had any indication of containing more than one active Na^+ channel. This was verified by inspecting several thousand consecutive traces at pulses to −40 mV or more positive test potentials up to +20 mV to identify any superimposition of opening events. Amplitude-histograms were formed after eliminating the transition points with the variance-mean technique introduced by Patlak (1988). Histograms of the open-channel lifetime were determined by using the baseline-method (Benndorf, 1995). For curve-fitting, a derivative-free Levenberg-Marquardt routine (Brown and Dennis, 1972) was used. Recording and analysis was performed on a PC-80386 and PC-80486, respectively, with the ISO2 software (MFK Computer, Niedernhausen, Germany).

RESULTS

Fig. 1 shows single-channel current traces at three different potentials from a channel (patch 1) that was exclusively gating in the normal, fast-inactivating mode (F mode). The maximum number of openings per depolarization was 4 at −60 mV, 2 at −30 mV, and 1 at 0 mV in ~1000 traces at each potential. The ensemble-averaged currents are shown on top. The fast time course of activation and inactivation yields a transient current, which is completed at −60 mV after ~3 ms, at −30 mV after ~1 ms, and at 0 mV after ~0.5 ms, with respect to the pulse beginning.

In Fig. 2 (*left*), the mean open time of the channel in the F mode was determined at the indicated three voltages (patch 1). All distributions could be fitted with a single exponential. The mean open time (τ_o) showed a bell-shaped voltage dependence (Yue et al., 1989; Benndorf and Koopmann, 1993), being 0.07 ms at −60 mV, 0.14 ms at −30 mV, and 0.08 ms at 0 mV. In the right column of Fig. 2, the cumulative first latency, not corrected for lag due to the clamp and the filter, is shown. The probability of nonempty traces increased from 30% at −60 mV to 70% at −30 mV and then decreased to 56% at 0 mV. This decline may be interpreted either by augmentation of a direct transition from the resting to the inactivated state at more positive potentials (Aldrich et al., 1983) or by more missed low-level opening events at this relative positive potential. The time before which half of the first channel openings occurred ($t_{0.5}$), referring only to traces with openings, declined from 0.58 ms at −60 mV to 0.14 ms at 0 mV. The unfortunate time calibration in Fig. 2 was chosen to facilitate comparison with the other modes illustrated below.

A transition from the F mode to the P mode is shown in Fig. 3. In this patch (patch 2), during most of the time a mixture of modes, including at least the F, M1, M2, and P mode was observed (cf Böhle and Benndorf, 1995). For a short time interval, which included 640 traces, only the F mode was present (−40 mV). The ensemble-averaged current is shown in the left of Fig. 3 *A*, and right beside the

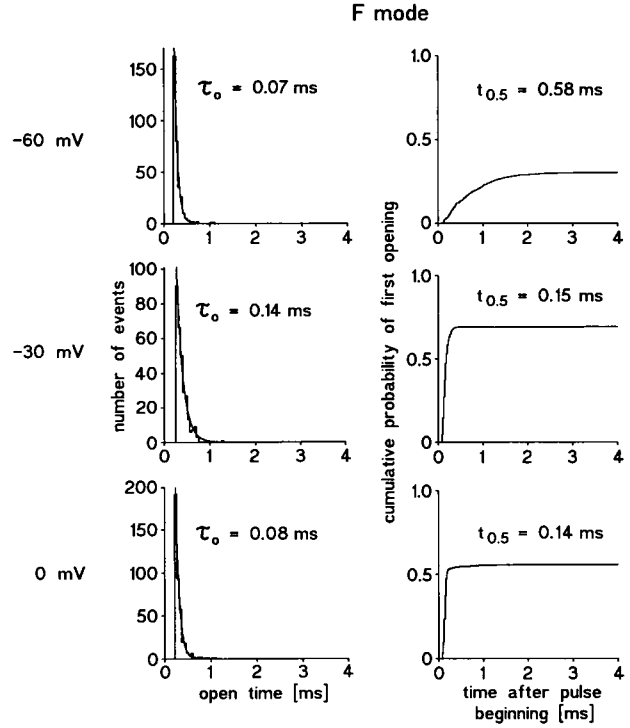

FIGURE 2 Histograms of the open-channel life time (*left*) and cumulative first-latency distributions (*right*) in the F mode at three different potentials (1016 traces at −60 mV, 1019 traces at −30 mV, and 1001 traces at 0 mV). The data could be fitted monoexponentially yielding the mean open times τ_0 as indicated (filter 10 kHz; baseline method; binwidth 50 μs). In the cumulative first-latency distributions, the probability of traces with either one or more openings was 30% at −60 mV, 70% at −30 mV, and 56% at 0 mV. The respective time before which half of the first channel openings occurred ($t_{0.5}$, referred only to traces with openings) is indicated (filter 5 kHz, threshold 60%, binwidth 20 μs).

long-time course of the averaged current per trace. Here each point represents the averaged current in a 4-ms interval. These plots are called henceforth "average-of-interval-plots." Eighteen minutes later, over the time in which 501 traces were recorded, exclusively the P mode was present at the same voltage of −40 mV. The amplitude of the ensemble-averaged current in the P mode (*right*) was about the same as in the F mode, but inactivation was dramatically slowed or even removed.

It might be argued that the changed kinetics was caused by an alteration of the voltage across the channel. At least across the pore, we could rule out a change of the driving force, because this was constant during the time interval of 18 min, as illustrated in Fig. 3 *B*. Here amplitude histograms in the F mode (*left*) and in the P mode (*right*) were formed (−40 mV), and each distribution was fitted with two Gaussian curves. The mean open-channel current amplitude in the F mode (2.307 pA) and in the P mode (2.342 pA) was equal. For comparison, with a single-channel conductance of 25 pS, an alteration of −40 mV would have produced a change in the single-channel current amplitude of −1 pA. This result excludes a slow voltage drift in our recording. It should be noted that heterogenous levels of single-channel currents were present (Benndorf, 1993, 1994) in both the F and the P modes. Of further interest is the observation that in the P mode the SD of the open-channel level clearly exceeded that in the baseline noise, whereas in the F mode the SD of the open channel level was similar to that of the baseline noise. This shows that the P mode contained more heterogeneous levels (T. Böhle and K. Benndorf, unpublished data).

In the P mode, directly before recording the traces at −40 mV, pulses to −60 mV were applied. Here only a few openings were observed, yielding the flat ensemble-averaged current on the top right in Fig. 3 *A*. Two minutes after recording at −40 mV, the Na^+ channel still acting in the P mode was pulsed to −20 mV (*lower right* part in Fig. 3 *A*). Here slow inactivation turned out during depolarization.

Although the P mode could also develop slow inactivation, it could be differentiated easily from the S mode by the different amplitudes of the plateau-like patterns in the average-of-interval-plot (Fig. 4; patch 3; −40 mV). Each number (1–10) refers to an interval of continuous recording in which the same prepulse was applied. Switching was independent of the prepulse potential. During the time interval of 1 min between blocks 1 and 2, the channel switched among the P, S, and M1 modes (see Böhle and Benndorf, 1995). In Fig. 4 *B*, 10 typical consecutive single-channel current traces, with the channel being in the S and the P mode, respectively, are shown. The S mode was dominated by long-lasting channel openings, which started promptly after the pulse beginning. In the P mode, openings did not start promptly after the pulse beginning and were short. Here sublevels appeared frequently, which may also be unresolved fast flickering. The second trace in the S mode might either be a sublevel (or an unresolved flicker in this mode) or a short period in another mode, e.g., the P mode, for which occurrence of lower levels is much more typical than for the S mode. The number of openings per trace in the S mode and the P mode was similar (see also Discussion).

Fig. 5 compares the S mode with the P mode at various potentials (patch 3). At −60 mV (*left*), two different ensemble-averaged currents in the S mode are superimposed; the one that was recorded first is dotted, and the other drawn as a line. In both currents, a second peak is clearly separated from the first. The recordings were 16 min apart. The coincidence of the courses indicates stability of the clamp. The plot of the time course of the averaged current per trace (*upper row, middle-left*) corresponds to that ensemble-averaged current, which was recorded second. When recording 27 min later, the same channel was gating by chance in the P mode (*upper row, right*). Here the ensemble-averaged current is of small amplitude (−60 mV, *outer right*) and activation is extremely slow. At −40 mV, again two different ensemble-averaged currents in the S mode are superimposed. They stem from two blocks of continuous recording, which were 1 min apart. The line-drawn one corresponds to that part of block 1 in Fig. 4 *A*, where the

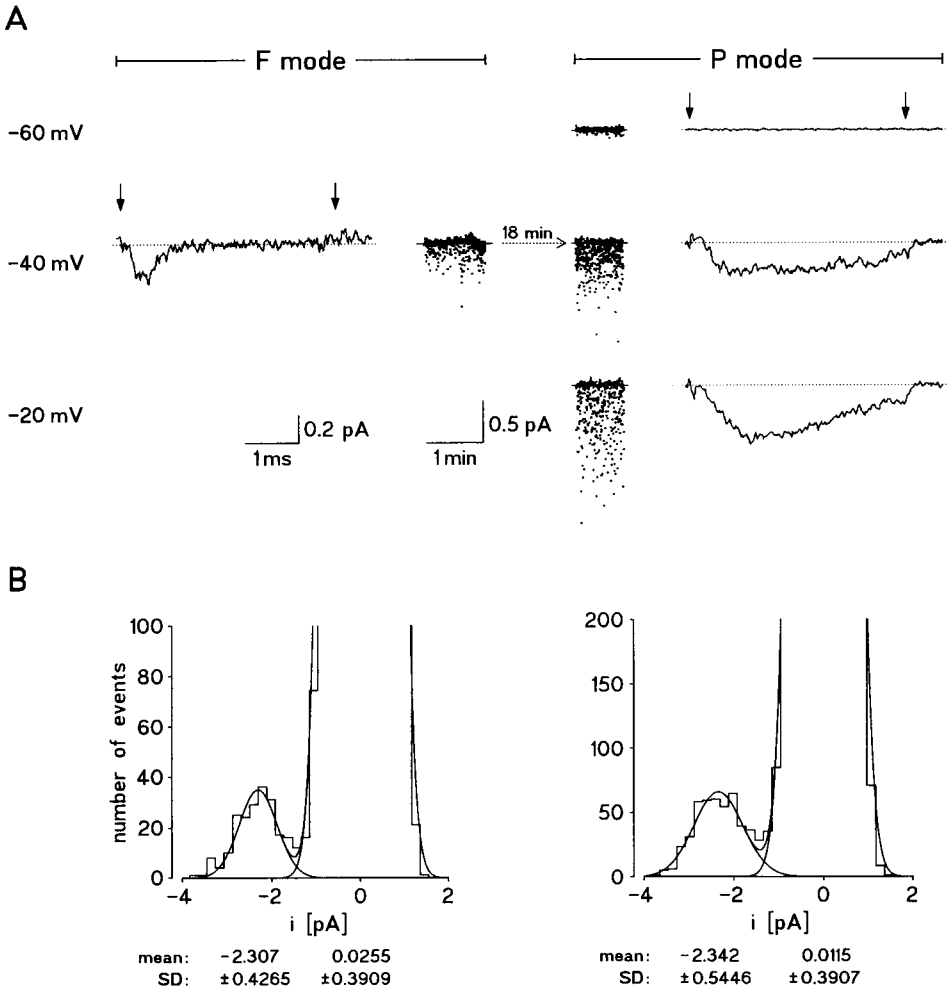

FIGURE 3 Slow transition from the F mode to the P mode during a time interval of ~18 min (patch 2, pipette resistance 42 MΩ; seal resistance 800 GΩ; F mode, 640 traces at −40 mV; P mode, 498 traces at −60 mV, 501 traces at −40 mV, 499 traces at −20 mV). (*A*) Ensemble-averaged currents (*lines*, outer left and outer right; filter 5 kHz; the arrows indicate beginning and end of the test pulses) and long-time courses of the averaged current per trace (*dots*, middle-left and middle-right; filter 20 kHz; every dot represents the averaged current of an individual trace of 4-ms duration) at different potentials. (*B*) Absence of any change in the electrochemical driving force during the slow transition from the F mode to the P mode. Two amplitude histograms at −40 mV are presented and each distribution was fitted with the sum of two Gaussian curves. The peak of the baseline noise is truncated and the parameters (mean, SD) are indicated (filter 20 kHz; window width for variance-mean analysis 75 μs; threshold variance 0.2 pA^2).

channel was in the S mode, and the dotted one corresponds to block 2 in Fig. 4 *A*. The ensemble-averaged current at −40 mV in the right stems from that part of block 1 in Fig. 4 *A*, where the channel was in the P mode. In this patch, recording at −20 mV is available only in the S mode, which is shown at the bottom. The small band of "less-dotted area," indicated by the horizontal arrows in the average-of-interval-plots, is explained in Discussion.

In Fig. 6, open-time histograms were built from recordings in the S mode (patch 3) and in the P mode (patches 2 and 3). At −60 mV, the mean open time was 0.42 ms in the S mode and 0.07 ms in the P mode. At −40 mV, two mean open times were present in the S mode (τ_{o1} = 1.01 ms, τ_{o2} = 0.13 ms). τ_{o2} equals the mean open time in the P mode at −40 mV (τ_o = 0.13 ms; right), suggesting that in the S mode a small portion of P mode was hidden. At −20 mV in the S mode, τ_{o1} (1.07 ms) was nearly unaltered with respect to τ_{o1} at −40 mV, whereas τ_{o2} (0.22 ms) increased. The mean open time found in the P mode at −20 mV (τ_o = 0.31 ms) was recorded from a different patch (patch 2), which might be the reason for the fact that it does not match perfectly τ_{o2} in the S mode.

In Fig. 7, cumulative first-latency distributions are plotted for the S mode (patch 3) and the P mode (patch 2). The pulse potential and the time ($t_{0.5}$) before which half of the first channel openings occurred are illustrated in the diagrams. In the S mode, $t_{0.5}$ declined from 1.61 ms at −80 mV to 0.32 ms at −40 mV and in the P mode from 2.14 ms at −60 mV to 0.37 ms at 0 mV.

In Fig. 8 *A* (patches 1, 2, 3, and 4), $t_{0.5}$ is plotted as function of the pulse potential for all three modes investigated in this study. Although $t_{0.5}$ in the F mode is very similar to the S mode at voltages between −60 and −20 mV, that of the P mode differs substantially from both of them being shifted to more positive potentials. The symbols in this plot were chosen such that they match the following plots (Figs. 8 *B* and 9). In detail, each mode is represented by a characteristic symbol (square, triangle, diamond), and the different patches are indicated by a characteristic filling. In Fig. 8 *B* (patches 1, 2, 3, and 4), the mean open time as function of the pulse potential is illustrated. In the S mode, τ_o increases at stronger depolarization up to −30 mV. At −20 mV, the mean open time is not prolonged further. The voltage dependence of τ_o in the P mode is shifted to the right in comparison with that in the S mode. In contrast to the results in Fig. 8 *A*, here the F mode is very similar to the P mode in the voltage range between −60 and −40 mV. In the F mode

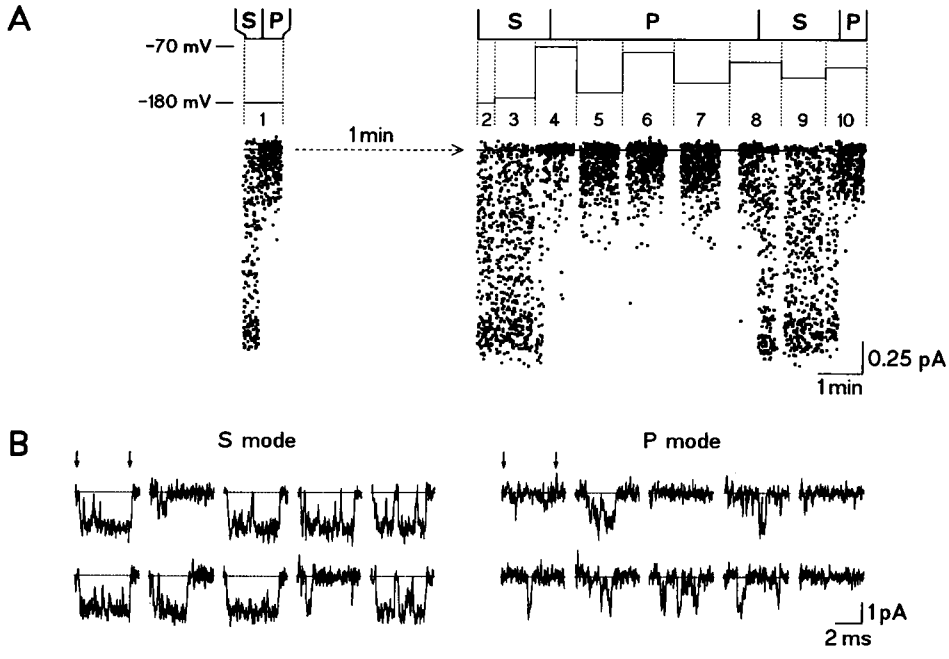

FIGURE 4 Comparison between currents in the S mode and in the P mode (patch 3, pipette resistance 97 MΩ; seal resistance 1000 GΩ; test pulse potential −40 mV). (*A*) Fast and repetitive switches between the S and P mode identified by plots of the long-time course of the averaged current per 4-ms trace. Ten numbered blocks of continuous recording each are shown. Switching was independent of the prepulse potential, which is indicated schematically (filter 20 kHz; 4224 traces; prepulse potential −180 mV (blocks 1, 2), −170 mV (block 3), −160 mV (block 5), −140 mV (block 7), −130 mV (block 9), −110 mV (block 10), −100 mV (block 8), −80 mV (block 6), −70 mV (block 4)). (*B*) Ten consecutive single-channel current traces in the S (*left*) and the P mode (*right*) from block 1 in part A (prepulse potential −180 mV; filter 5 kHz; the arrows indicate beginning and end of the test pulses).

at more depolarized potentials, τ_o is getting shorter again, as expected from the increasing effect of inactivation (Yue et al., 1989; Benndorf and Koopmann, 1993).

In Fig. 9 (patches 1, 2, 3, and 4), steady-state activation curves for the three different modes are shown. They were obtained by fitting a Boltzmann distribution to the respective data points in each mode. In part *A*, the voltage of half-maximum activation ($v_{0.5}$) and the slope factor (k) are indicated in each diagram. In part *B*, the three curves are superimposed for better comparison. The F mode yielded the steepest and the P mode the most flat curve. Half-maximum steady-state activation was at most negative potentials in the S mode and at most positive potentials in the P mode.

DISCUSSION

The F, S, and P mode may be identified by characteristic voltage dependence of τ_o, $t_{0.5}$, and steady-state activation

Three modes of Na^+ channel action, the normal, fast-inactivating F mode, the slowly inactivating S mode, and the persistent P mode, as termed from differentiation at −40 mV in our previous report (Böhle and Benndorf, 1995), were investigated at different potentials. Voltage dependence of three parameters was determined: 1) steady-state activation, 2) the cumulative first-latency distribution, and 3) the mean open-time distribution. The unaltered mean single-channel current amplitude in the different modes over the time of the experiment excludes any masked alteration in the electrochemical driving force for Na^+ across the channel pore. Hence, voltage shifts at the pipette or alterations in the concentration of Na^+ on either side of the membrane are certainly not the cause of the observed changes in Na^+-current kinetics. Characteristic variability in the voltage dependence of the three parameters was found: half-maximum activation ($v_{0.5}$) in the F mode was positioned at about −48 mV, whereas in the S mode it was shifted to more negative voltages for ~13 mV and in the P mode to more positive voltages for ~33 mV. Concomitantly, the slope of both curves decreased by a factor of

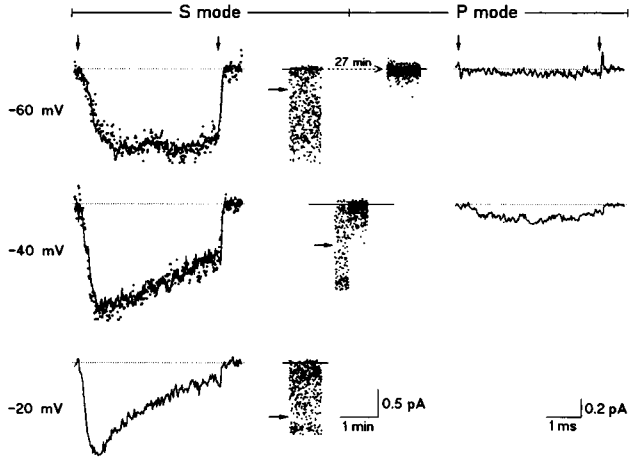

FIGURE 5 Currents of the S mode and the P mode at different potentials (patch 3, S mode: 501 and 502 traces at −60 mV, 208 and 215 traces at −40 mV, 502 traces at −20 mV; P mode: 511 traces at −60 mV, 300 traces at −40 mV). Ensemble-averaged currents are shown in the outer left and outer right. At −60 and −40 mV in the S mode, two different ensemble-averaged currents are superimposed (filter 5 kHz; the vertical arrows indicate beginning and end of the test pulses). Long-time courses of the averaged current per 4-ms trace are shown in the middle (filter 20 kHz; the horizontal arrows indicate a small band of "less-dotted area").

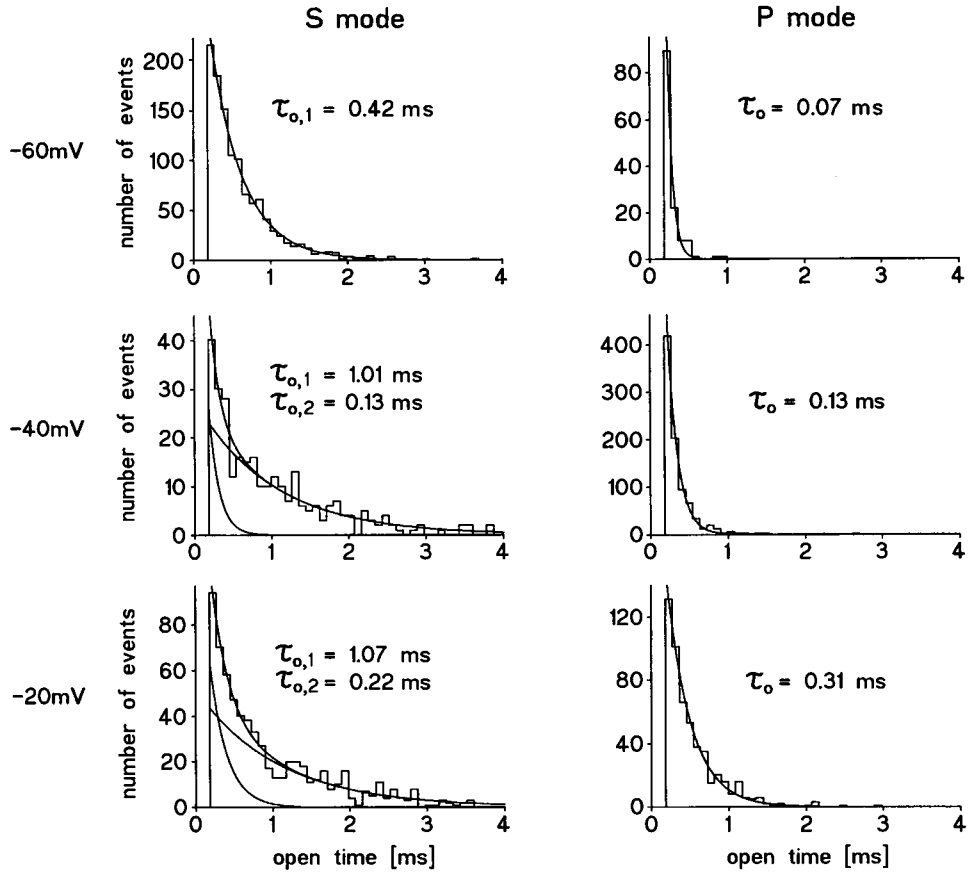

FIGURE 6 Histograms of the open-channel life time in the S mode and the P mode at different potentials (filter 10 kHz; baseline method; bin-width 90 μs; S mode, patch 3: 502 traces at −60 mV, 248 traces at −40 mV, 502 traces at −20 mV; P mode, patch 3: 511 traces at −60 mV, 1004 traces at −40 mV; P mode, patch 2: 499 traces at −20 mV). The data could be fitted monoexponentially in the P mode at all potentials and in the S mode at −60 mV, and biexponentially in the S mode at −40 and −20 mV. The mean open-times τ_o are indicated in each diagram.

~1.5 (S mode/F mode) and ~1.8 (P mode/F mode). Compared with the F mode, the voltage dependence of $t_{0.5}$, as determined from the cumulative first latency in the P mode, was shifted by 45–55 mV to more positive potentials, whereas in the S mode, it was similar at potentials between −60 and −20 mV. The voltage dependence of the open-channel life time in the S mode was shifted for ~25–40 mV to more negative potentials with respect to that in the F mode at voltages between −60 and −40 mV. In this potential range, the mean open time in the F mode was similar to the P mode. At more positive voltages, τ_o in the F mode was clearly shorter than in the P mode, which suggests contribution of more inactivation in the F mode. Because the S mode at voltages up to −30 mV and the P mode up to 0 mV showed a monotonous prolongation of the mean open time, it is assumed that at these voltages deactivation preferentially determines τ_o. In the S mode, the cessation at −30 mV of the monotonous incline of τ_o might be caused by an increasing effect of inactivation.

The results are summarized in Table 1. Herein, steady-state activation is characterized by the half-maximum value ($v_{0.5}$) and the slope (k), the voltage dependence of the first latency by that voltage, at which $t_{0.5}$ is 0.5 ms, and the voltage dependence of the mean open time by that voltage, at which τ_o is 0.12 ms. The second value for the voltage of the mean open time in the F mode results from a bell-shaped voltage dependence (Yue et al., 1989; Benndorf and Koopmann, 1993) and reflects the increasing contribution of inactivation. From Table 1, it becomes obvious that the transition from the S mode to the P mode, as observed in patch 3, is accompanied in all three parameters by a concerted alteration, i.e., a large shift to more positive voltages. In contrast, the transition from the F mode to the P mode, as observed in patch 2, is accompanied by a differentiated alteration: $t_{0.5}$ and steady-state activation considerably shift to more positive voltages, whereas τ_o nearly does not shift (in the F mode, τ_o preferentially determined by deactivation is compared; left value). These different results may be grounded on the different types of transition between the modes as observed in the experiments: transitions from the S mode to the P mode were instantaneous and reversible, whereas the transition from the F mode to the P mode was a slow process in which different intermediate modes and, possibly, also a mixture of modes had appeared, leading to a progressive loss of inactivation during the experiment (see Böhle and Benndorf, 1995).

The small amount of P mode inherent in the S mode

In our previous paper (Böhle and Benndorf, 1995), it was suggested that in the S mode a small portion of P mode always was included. A closer look at the average-of-inter-

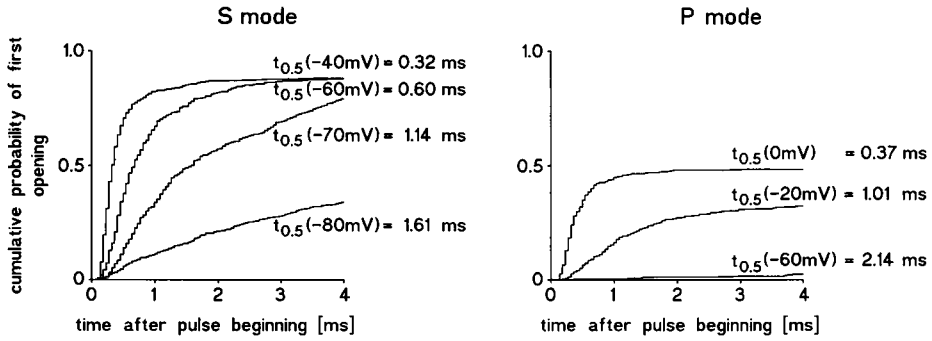

FIGURE 7 Cumulative first-latency distributions in the S mode (*left*) and the P mode (*right*) at different potentials (filter 5 kHz; threshold 60%; bin-width 45 μs; S mode, patch 3: 503 traces at −80 mV, 507 traces at −70 mV, 502 traces at −60 mV, 589 traces at −40 mV; P mode, patch 2: 498 traces at −60 mV, 499 traces at −20 mV, 500 traces at 0 mV). The time before which half of the first channel openings occurred ($t_{0.5}$, referred only to traces with openings) is indicated for each potential in the two diagrams.

val-plots in Fig. 5 (see horizontal arrows) suggests that in the S mode a small band of "less-dotted area" moves downward from a low current level to a higher current level when depolarization is augmented. The area of lower channel activity with respect to the small band of "less-dotted area" might correspond to the P mode, as also the dots of the P mode at −60 and −40 mV suggest. In these plots, the averaged current per trace is generally proportional to the number, the amplitude, and the duration of openings within the 4-ms interval of a single trace. With stronger depolarization, the number of openings per trace decreases, as does the single-channel current amplitude (see F mode, Fig. 1), but in the P mode the mean open time increases. This overbalances the other two parameters and leads to an increase of the area tentatively attributed to the P mode.

The ensemble-averaged currents in the S mode revealed a biphasic time course of inactivation, which is explained by the small amount of P mode inherent in the S mode. This is most prominent at −60 mV (see Fig. 5), where the slow first latency of the P mode ($t_{0.5}$ = 2.14 ms) combined with inactivation after the peak of the S mode easily may generate a second peak. If a small amount of P mode is hidden in the S mode, one should see two different mean open times, which was indeed found at −40 and −20 mV. At −60 mV, only the slow time constant of the S mode was resolved, which may have two reasons: 1) the steady-state

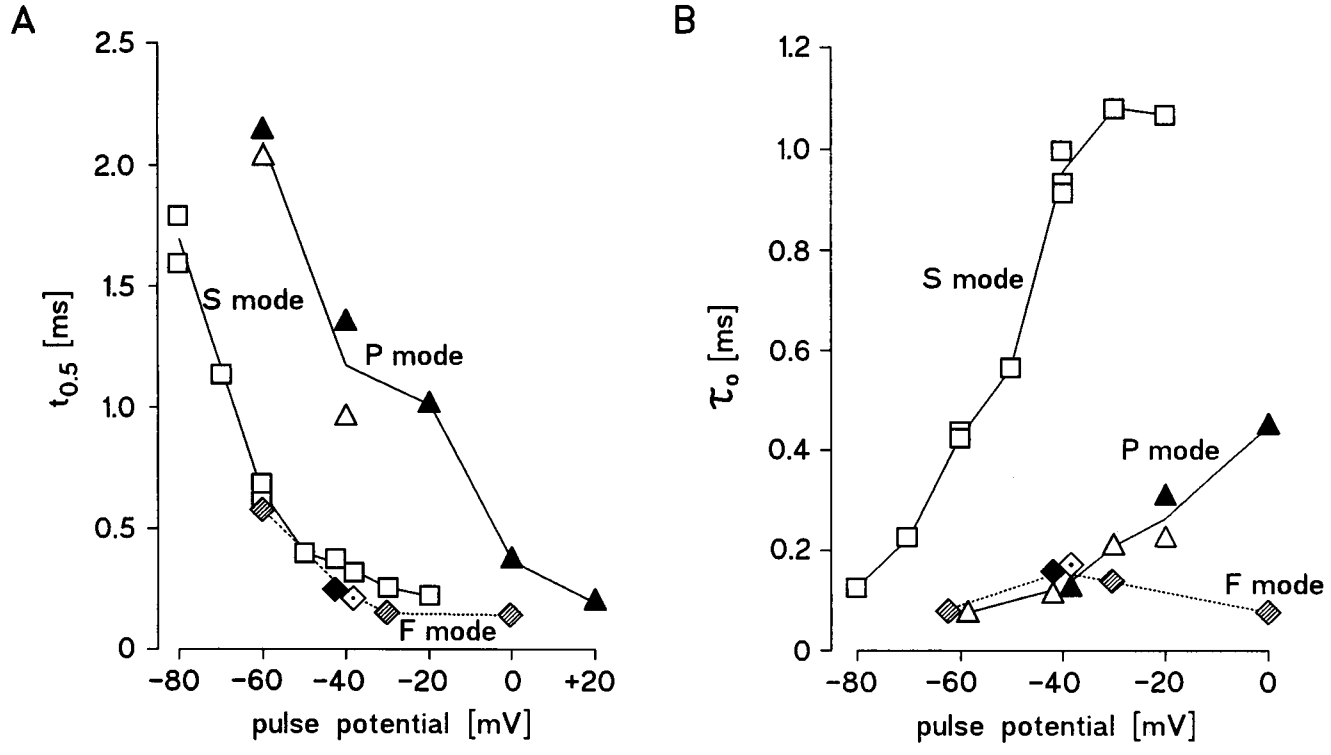

FIGURE 8 Voltage dependence of first latency (*A*, ordinate: $t_{0.5}$) and mean open time (*B*, ordinate τ_o) in the F mode (patch 1; patch 2; patch 4: pipette resistance 17 MΩ, seal resistance 27 GΩ, prepulse potential −100 mV), the S mode (patch 3), and the P mode (patches 2 and 3). For each mode, a characteristic type of symbol was chosen, different filling of the symbols indicates different patches, and the symbols match in *A* and *B*. In *B* at −80 mV (S mode), data were lumped from traces in two different blocks of continuous recording, which were 16 min apart. The lines connecting the data points are drawn continuous for the S mode and the P mode and stippled for the F mode.

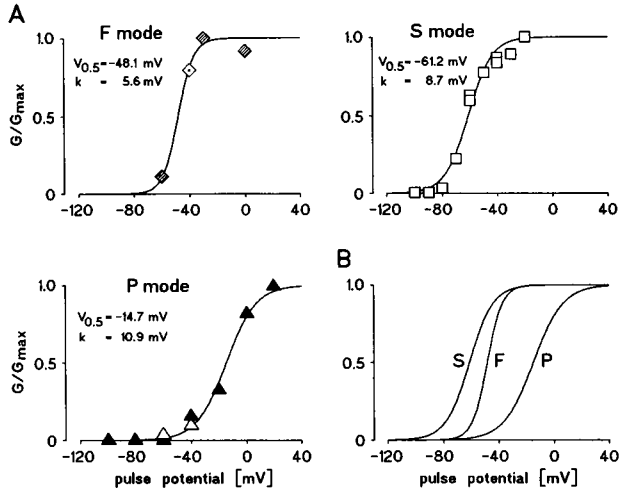

FIGURE 9 Voltage dependence of steady-state activation in the F mode (patches 1 and 4), the S mode (patch 3), and the P mode (patches 2 and 3). (*A*) Boltzmann fit to the data points in the different modes. Symbols correspond to Fig. 8. The voltage of half-maximum activation ($V_{0.5}$) and the slope factor (k) for each mode is indicated. (*B*) Superimposed Boltzmann fits of the three diagrams in A.

activation curves reveal that at −60 mV only ~2% of the channel in the P mode and ~55% of the channel in the S mode is activated; 2) the average-of-interval-plot illustrates that at −60 mV in the S mode, the portion of the P mode is very small, i.e., only a little amount of P mode is hidden in the S mode. Thus, the fast time constant of the P mode at −60 mV is not resolved.

When comparing the number of openings per trace in the P and the S mode, there was no significant difference (Fig. 4 *B*). The *exact* number of openings per trace in each of both modes is difficult to define for two reasons: 1) the small portion of P mode inherent in the S mode, and 2) the fast flicker and the frequent occurrence of heterogeneous levels in the P mode. As a consequence of the second reason, any determination of the number of openings per trace would depend to a high degree upon the filter-band width. Because with short test pulses of only 4-ms duration, as used here, the number of openings per trace is not altered notably by the switching between the S and the P mode, and being aware of the limitations in the resolution of short events, this type of analysis was omitted.

TABLE 1 Voltage at specified values of the parameters $t_{0.5}$, τ_o, and steady-state activation in three different modes of Na^+ channel action

Parameter	F mode	S mode	P mode
Steady-state activation			
$v_{0.5}$	−48 mV	−61 mV	−15 mV
k	6 mV	9 mV	11 mV
First latency			
$v(t_{0.5} = 0.5$ ms)	−56 mV	−54 mV	−4 mV
Mean open time			
$v(\tau_o = 0.12$ ms)	−48 mV/−24 mV	−80 mV	−43 mV

Possible alterations of the channel protein leading to mode switches

The question arises: Which parts of the gating machinery are altered in the different modes? The native brain Na^+ channel is a heterotrimeric protein consisting of an α, a β_1, and a disulphide-linked β_2 subunit (Catterall, 1992). In skeletal muscle and heart, besides an α, a β_1 subunit of the Na^+ channel has been identified only (Makita et al., 1994). The pore-forming α subunit contains four homologous domains (I–IV), and each domain comprises six transmembrane α helices (S1–S6). Of particular interest for the process of activation is the S4 segment of each homologous domain, which contains a positively charged residue at every third amino acid position. Upon depolarization, an outward movement of positive charges is measurable as a gating current, which precedes opening of the Na^+ channel. Point mutations in the S4 segment yielded that the slope of the activation curve is correlated to the amount of charged groups in S4 (Stühmer et al., 1989).

Two different types of inactivation, which are independent of each other, are found in Na^+ channels, namely, fast inactivation and slow inactivation. According to Armstrong and Bezanilla (1977), fast inactivation depends on a structure on the channel's cytoplasmic side that can block ionic movements by plugging the open pore once a sufficient fraction of the activation gates has moved out of its way. It is assumed that an intracellular loop between homologous domains III and IV is involved in this process (Vassilev et al., 1988, 1989; Stühmer et al., 1989). Slow inactivation has a separate voltage dependence (Ruff et al., 1988), and it remains functional even when fast inactivation has been removed (Rudy, 1978; Patlak and Ortiz, 1986; Quandt, 1987). Recent results from brain Na^+ channels (Isom et al., 1992) show that high-frequency activity is inhibited in the absence of the β_1 subunit, suggesting that this subunit is involved in slow inactivation.

The voltage dependence of steady-state activation and of $t_{0.5}$ from the cumulative first latency in the present study clearly refers to the activation process. The voltage dependence of the mean open time may be influenced by the deactivation *and* inactivation processes. A mode switch might be the consequence of 1) an alteration of the voltage-sensing mechanisms or 2) a voltage-independent alteration of the channel. The observed differences in the slope of steady-state activation between the modes may be explained by an alteration in the voltage sensor, which conflicts, however, with the independence of mode switches of the prepulse potential, as shown in Fig. 4 *A*. The diverse shifts in the voltage dependence of steady-state activation, $t_{0.5}$, and τ_o (τ_o preferentially determined by deactivation is compared) may be explained by an alteration in the voltage sensor or in a voltage-independent step. The observed differences in the mean open time at less negative voltages may be attributed to alterations in fast inactivation.

The observed variability among the modes might be caused by regulatory processes involving phosphorylation.

Na^+ channels in the heart and the brain are substrates for phosphorylation by both protein kinase A (PKA) (Sunami et al., 1991; Ono et al., 1993; Costa and Catterall, 1984; Costa et al., 1982; Rossie and Catterall, 1987) and protein kinase C (PKC) (Costa and Catterall, 1984; Murphy and Catterall, 1992). Putative phosphorylation sites for PKA-phosphorylation are located in the intracellular loops between segments I and II and for PKC-phosphorylation in the intracellular loops between segments III and IV, but also between I and II. Although differential effects were shown for the distinct phosphorylation sites, recent results (Li et al., 1993) demonstrate a convergent regulation of the Na^+ channel by PKC and PKA. In myocardial Na^+ channels, phosphorylation by PKA induced a shift of the availability and the conductance in the hyperpolarizing direction (Ono et al., 1993). In the same tissue, the catalytic subunit (C subunit) of PKA decreased the peak averaged current and slowed the current decay (Sunami et al., 1991), effects that were caused by a decrease in the open probability and an increase in the first latency. Also, oxidation might be considered as a cause of modal behavior, because it is known that fast inactivation in a mammalian voltage-dependent $I_K(A)$ channel is regulated by cysteine oxidation (Ruppersberg et al., 1991). Other possible regulatory processes involving intracellular Ca^{2+} (Egger and Greef, 1994) or cytoskeleton (Cantiello et al., 1991), and also mechanical actions on the plasma membrane within the extraordinarily tipped patch pipettes (Sokabe et al., 1991; Böhle and Benndorf, 1994), have been discussed in our previous report (Böhle and Benndorf, 1995).

In the same study, we showed that transitions took place mainly between adjacent modes, i.e., between modes that differ only slightly in macroscopic inactivation kinetics. If this mode-switch behavior is valid in general, then under physiological conditions a direct transition from the F mode to the P mode would be unlikely. Hence, the slow transition from the F mode to the P mode cannot be explained by a single mechanism, but only as the result of a series of switches between adjacent modes. Each type of switch might alter an individual rate constant in the reaction scheme among closed, open, and inactivated states. This model of switching between adjacent modes only is not in contradiction to the action of a series of drugs, which dramatically change inactivation kinetics from fast to nearly complete absence of inactivation, as lysophosphatidylcholine (LPC) (Burnashev et al., 1989) or to complete absence of inactivation as DPI-201-106 (Kohlhardt et al., 1987). Either these drugs act in a rather nonspecific fashion, thereby altering several mechanisms simultaneously, and in this way skipping the physiologically possible way of switching between modes, or the respective drugs produce new modes. Of certain interest might be the drug LPC, which induces long-lasting bursts of Na^+ channel openings. As LPC, a product of phospholipid catabolism, is accumulated in the ischemic myocardium (Corr et al., 1978, 1979, 1982), during ischemia a Na^+-channel mode might be uncovered, which is not present under physiological conditions. Because sustained Na^+ influx leads to a harmful increase of the Ca^{2+} concentration via the Na^+/Ca^{2+} exchanger, the switch to slowly or not inactivating modes might be of importance for the ischemia-induced cell death.

We thank D. Metzler and R. Kemkes for excellent technical assistance and R. Koopmann for carefully reading the manuscript.

REFERENCES

Aldrich, R. W., D. P. Corey, and C. F. Stevens. 1983. A reinterpretation of mammalian sodium channel gating based on single channel recording. *Nature*. 306:436–441.

Armstrong, C. M., and F. Bezanilla. 1977. Inactivation of the sodium channel. II. Gating current experiments. *J. Gen. Physiol.* 70:567–590.

Attwell, D., I. Cohen, D. Eisner, M. Ohba, and C. Ojeda. 1979. The steady-state TTX-sensitive ("window") Na current in cardiac Purkinje fibers. *Pflügers Arch.* 379:137–142.

Benndorf, K. 1993. Multiple levels of native cardiac Na^+ channels at elevated temperature measured with high-bandwidth/low-noise patch clamp. *Pflügers Arch.* 422:506–515.

Benndorf, K. 1994. Properties of single cardiac Na channels at 35°C. *J. Gen. Physiol.* 104:801–820.

Benndorf, K. 1995. Low noise recording. *In* Single Channel Recording, 2nd ed. B. Sakmann and E. Neher, editors. Plenum Press, New York. 129–145.

Benndorf, K., and R. Koopmann. 1993. Thermodynamic entropy of two conformational transitions of single Na^+ channel molecules. *Biophys. J.* 65:1585–1589.

Benndorf, K., and B. Nilius. 1987. Inactivation of sodium channels in myocardial mouse cells. *Eur. Biophys. J.* 15:117–127.

Böhle, T., and K. Benndorf. 1994. Facilitated giga-seal formation with a just originated glass surface. *Pflügers Arch.* 427:487–491.

Böhle, T., and K. Benndorf. 1995. Multimodal action of single Na^+ channels in myocardial mouse cells. *Biophys. J.* 68:121–130.

Brown, A. M., K. S. Lee, and T. Powell. 1981. Sodium currents in single rat heart muscle cells. *J. Physiol.* 318:479–500.

Brown, K. M., and J. E. Dennis, Jr. 1972. Derivative-free analogues of the Levenberg-Marquardt and Gauss algorithms for nonlinear least squares approximation. *Num. Math.* 18:289–297.

Burnashev, N. A., A. I. Undrovinas, I. A. Fleidervish, and L. V. Rosenshtraukh. 1989. Ischemic poison lysophosphatidylcholin modifies heart sodium channels gating inducing long-lasting bursts of openings. *Pflügers Arch.* 415:124–126.

Cachelin, A. B., J. E. Peyer, S. Kokubun, and H. Reuter. 1983. Sodium channels in cultured cardiac cells. *J. Physiol.* 340:389–401.

Cantiello, H. F., J. L. Stow, A. G. Prat, and D. A. Ausiello. 1991. Actin filaments regulate epithelial Na^+ channel activity. *Am. J. Physiol.* 261: C882–C886.

Carmeliet, E. 1984. Slow inactivation of the sodium current in rabbit cardiac Purkinje fibres. *J. Physiol.* 353:125*a* (Abstr.).

Carmeliet, E. 1987. Slow inactivation of the sodium current in rabbit cardiac Purkinje fibres. *Pflügers Arch.* 408:18–26.

Catterall, W. A. 1988. Structure and function of voltage-sensitive ion channels. *Science.* 242:50–61.

Catterall, W. A. 1992. Cellular and molecular biology of voltage-gated sodium channels. *Physiol. Rev.* 72: S15–S48.

Corr, P. B., M. E. Cain, F. X . Witkowski, D. A. Price, and B. E. Sobel. 1979. Potential arrhythmogenic electrophysiological derangements in canine Purkinje fibres induced by lysophosphoglycerides. *Circ. Res.* 44:822–832.

Corr, P. B., R. W. Gross, and B. E. Sobel. 1982. Arrhythmogenic amphiphilic lipids and the myocardial cell membrane. *J. Mol. Cell. Cardiol.* 14:619–626.

Corr, P. B., F. X . Witkowski, and B. E. Sobel. 1978. Mechanisms contributing malignant disrhythmias induced by ischemia in the cat. *J. Clin. Invest.* 61:109–119.

Costa, M. R., J. E. Casnellie, and W. A. Catterall. 1982. Selective phosphorylation of the α subunit of the sodium channel by cAMP-dependent protein kinase. *J. Biol. Chem.* 257:7918–7921.

Costa, M. R., and W. A. Catterall. 1984. Cyclic-AMP-dependent phosphorylation of the α subunit of the sodium channel in synaptic nerve ending particles. *J. Biol. Chem.* 259:8210–8218.

Costa, M. R., and W. A. Catterall. 1984. Phosphorylation of the α subunit of the sodium channel by protein kinase C. *Cell. Mol. Neurobiol.* 4:291–297.

Egger, M., and N. G. Greef. 1994. Modulation of the number of activatable Na^+ channels by $[Ca^{2+}]_i$ and a phosphatase blocker. *Biophys. J.* 66:203*a* (Abstr.).

Grant, A. O., C. F. Starmer, and H. C. Strauss. 1983. Unitary sodium channels in isolated cardiac myocytes of rabbit. *Circ. Res.* 53:823–829.

Isom, L. L., K. S. De-Jongh, D. E. Patton, B. F. Reber, J. Offord, H. Charbonneau, K. Walsh, A. L. Goldin, and W. A. Catterall. 1992. Primary structure and functional expression of the $\beta 1$ subunit of the rat brain sodium channel. *Science.* 256:839–842.

Kohlhardt, M., U. Fröbe, and J. W. Herzig. 1987. Properties of normal and non-inactivating single cardiac Na^+ channels. *Proc. R. Soc. Lond. B.* 232:71–93.

Kunze, D. L., A. E. Lacerda, D. L. Wilson, and A. M. Brown. 1985. Cardiac Na^+ currents and the inactivating, reopening, and waiting properties of single cardiac Na^+ channels. *J. Gen. Physiol.* 86:691–719.

Lee, K. S., T. A. Weeks, R. L. Kao, N. Akaike, and A. M. Brown. 1979. Sodium currents in single heart muscle cells. *Nature.* 278:269–271.

Li, M., J. W. West, R. Numann, B. J. Murphy, T. Scheuer, and W. A. Catterall. 1993. Convergent regulation of Na^+ channels by protein kinase C and cAMP-dependent protein kinase. *Science.* 261:1439–1442.

Liu, Y., L. J. DeFelice, and M. Mazzanti. 1992. Na channels that remain open throughout the cardiac action potential plateau. *Biophys. J.* 63: 654–662.

Makita, N., P. B. Bennett, Jr., and A. L. George, Jr. 1994. Voltage-gated Na^+ channel β_1 subunit mRNA expressed in adult human skeletal muscle, heart, and brain is encoded by a single gene. *J. Biol. Chem.* 269:7571–7578.

Mazzanti, M., and L. J. DeFelice. 1987. Na channel kinetics during the spontaneous heartbeat in chick ventricle cells. *Biophys. J.* 52:95–100.

Murphy, B. J., and W. A. Catterall. 1992. Phosphorylation of purified rat brain Na^+ channel reconstituted into phospholipid vesicles by protein kinase C. *J. Biol. Chem.* 267:16129–16134.

Numann, R., W. A. Catterall, and T. Scheuer. 1991. Functional modulation of brain sodium channels by protein kinase C phosphorylation. *Science.* 254:115–118.

Ono, K., H. A. Fozzard, and D. A. Hanck. 1993. Mechanism of cAMP-dependent modulation of cardiac sodium channel current kinetics. *Circ. Res.* 72:807–815.

Patlak, J. B. 1988. Sodium channel subconductance levels measured with a new variance-mean analysis. *J. Gen. Physiol.* 92:413–430.

Patlak, J. B. 1991. Molecular kinetics of voltage-dependent Na^+ channels. *Physiol. Rev.* 71:1047–1080.

Patlak, J. B., and M. Ortiz. 1985. Slow currents through single sodium channels of the adult rat heart. *J. Gen. Physiol.* 86:89–104.

Patlak, J. B., and M. Ortiz. 1986. Two modes of gating during late Na^+ channel currents in frog sartorius muscle. *J. Gen. Physiol.* 87:305–326.

Quandt, F. N. 1987. Burst kinetics of sodium channels which lack fast inactivation in mouse neuroblastoma cells. *J. Physiol.* 392:563–585.

Rossie, S., and W. A. Catterall. 1987. Cyclic-AMP-dependent phosphorylation of voltage-sensitive sodium channels in primary cultures of rat brain neuron. *J. Biol. Chem.* 262:12735–12744.

Rudy, B. 1978. Slow inactivation of the sodium conductance in squid giant axons: Pronase resistance. *J. Physiol.* 283:1–21.

Ruff, R. L., L. Simoncini, and W. Stühmer. 1988. Slow sodium channel inactivation in mammalian muscle: a possible role in regulating excitability. *Muscle Nerve.* 11:502–510.

Ruppersberg, J. P., M. Stocker, O. Pongs, S. H. Heinemann, R. Frank, and M. Koenen. 1991. Regulation of fast inactivation of cloned mammalian I_K(A) channels by cysteine oxidation. *Nature.* 352:711–714.

Sokabe, M., F. Sachs, and Z. Jing. 1991. Quantitative video microscopy of patch clamped membranes. Stress, strain, capacitance, and stretch channel activation. *Biophys. J.* 59:722–728.

Stühmer, W., F. Conti, H. Suzuki, X. Wang, M. Noda, N. Yahagi, H. Kubo, and S. Numa. 1989. Structural parts involved in activation and inactivation of the sodium channel. *Nature.* 339:597–603.

Sunami, A., Z. Fan, F. Nakamura, M. Naka, T. Tanaka, T. Sawanobori, and M. Hiraoka. 1991. The catalytic subunit of cyclic AMP-dependent protein kinase directly inhibits sodium channel activities in guinea-pig ventricular myocytes. *Pflügers Arch.* 419: 415–417.

Vassilev, P. M., T. Scheuer, and W. A. Catterall. 1988. Identification of an intracellular peptide segment involved in sodium channel inactivation. *Science.* 241:1658–1661.

Vassilev, P. M., T. Scheuer, and W. A. Catterall. 1989. Inhibition of inactivation of single sodium channels by a site-directed antibody. *Proc. Natl. Acad. Sci. USA.* 86:8147–8151.

Wellis, D., L. J. DeFelice, and M. Mazzanti. 1990. Outward Na current in beating heart cells. *Biophys. J.* 57:41–48.

Yue, D. T., J. H. Lawrence, and E. Marban. 1989. Two molecular transitions influence cardiac sodium channel gating. *Science.* 244: 349–352.